CEMCAP

Co-funded by the European Union

Grant Agreement Number:
641185

Action acronym:
CEMCAP

Action full title:
CO_2 capture from cement production

Type of action:

H2020-LCE-2014-2015/H2020-LCE-2014-1

Starting date of the action: 2015-05-01
Duration: 42 months

D7.2
Oxyfuel burner prototype performance tests
Revison 1

Due delivery date: 2017-10-15
Actual delivery date: 2018-07-16

Organization name of lead participant for this deliverable:
IFK, University of Stuttgart

Project co-funded by the European Commission within Horizon2020		
Dissemination Level		
PU	Public	X
CO	Confidential, only for members of the consortium (including the Commission Services)	

Deliverable number:	D7.2
Deliverable title:	Oxyfuel burner prototype performance tests
Work package:	WP 7 Oxyfuel burner technology
Lead participant:	USTUTT

Author(s)		
Name	**Organisation**	**E-mail**
*Francisco Carrasco M.	IFK, University of Stuttgart	francisco.carrasco@ifk.uni-stuttgart.de
Simon Grathwohl	IFK, University of Stuttgart	simon.grathwohl@ifk.uni-stuttgart.de
Jörg Maier	IFK, University of Stuttgart	joerg.maier@ifk.uni-stuttgart.de
Eike Wilms	thyssenkrupp Industrial Solutions AG	eike.willms@thyssenkrupp.com
Johannes Ruppert	VDZ gGmbH	johannes.ruppert@vdz-online.de

*Lead author

Keywords

Burner design, oxyfuel, pilot testing

Abstract

The report here presented serves a summary of the activities and findings related to the testing of the prototype oxyfuel burner in the 500 kW test facility. This document presents information on the design of the prototype burner, including the criteria and constraints considered for downscaling. Likewise, a description of the test facility and demonstration cases is made including carried out measurements. Furthermore, an interpretation of the measurements is done to understand the differences between air and oxyfuel firing experiments. This information has been used for validation of further analysis tools, including CFD and process simulations. Finally, assessments of the results as well as relevant conclusions are drawn from these investigations.

Please cite this report as: *Carrasco, Francisco; Grathwohl, Simon; Maier, Jörg; Wilms, Eike; Ruppert, Johannes. 2018. Oxyfuel burner prototype performance tests (D7.2).*
Refer to the CEMCAP community in Zenodo.org for citation with DOI.

TABLE OF CONTENTS

Page

This project has received funding from the European Union's Horizon2020 Research and Innovation Programme under Grant Agreement No 641185

1 INTRODUCTION

In the frame of the CEMCAP Project a number of CCS technologies are investigated with focus on their successful applicability to the cement production process. One of these researched technologies is oxy-fuel combustion. The concept of oxy-fuel involves the combustion in presence of oxygen and a portion of recirculated flue gases (mainly CO_2) instead of air. For a correct assessment of this technology in the clinker burning process the influence of a different combustion atmosphere (O_2/CO_2) on the heat transfer mechanisms in the kiln should be investigated.

Work package 7 is dedicated to experimental and numerical testing of a prototype oxy-fuel burner in the 500 kW_{th} combustion facility at University of Stuttgart. This report contains a summary of the results of a series of demonstrations tests at the 500 kWth combustion test rig at University of Stuttgart (USTUTT). A down-scaled kiln burner prototype designed in cooperation with ThyssenKrupp (TKIS) was previously manufactured by USTUTT and then employed for the combustion tests. The investigations were focused on comparing the combustion behavior of selected fuels (lignite, petcoke, SRF), in terms of temperature, heat flux and species profiles (CO_2, CO, O_2, NO_x, SO_2) under air and oxy-fuel conditions.

The results aim to be used as validation data for CFD simulations of additional oxy-fuel cases. Likewise, the results aim to be used qualitatively as information on input parameters in the oxy-fuel process modeling done in WP6.

This project has received funding from the European Union's Horizon2020 Research and Innovation Programme under Grant Agreement No 641185

2 BURNER DESIGN

2.1 Burner design requirements

Modern industrial size kiln sintering zone burners in cement rotary kilns are designed according process parameters like temperature, air flow rate and gas velocity as showed in Table 2.1. This information can be complemented with Table 2.2, which depicts the changes in gas composition under oxyfuel combustion. CFD simulations have been considered to derive the oxy-fuel burner requirements as described in a study made by the European Cement Research Academy [1]. The generic burner design described in [1] is similar to the design of commercial nozzle-type burners. Thus down-scaling and testing of a commercial nozzle-type kiln burner with high swirl number was considered a proper method to investigate its suitability for oxyfuel technology.

Table 2-1: Typical parameters for modern kiln sintering zone burners operated with air

Parameter	Primary air (through burner)	Secondary air (from cooler)
Temperature	40 – 60 °C	800 – 1100 °C
Air flow rate	6 - 10% (of combustion gas)	0.85 - 1 $m^3_N/kg_{clinker}$ (~90% of combustion gas)
Velocity	200 - 250 m/s (primary air exit velocity, nozzles) 15 - 20 m/s (cooling air/transport air)	~5 m/s (at burner tip)

Table 2-2: Oxy-fuel gas compositions and typical parameters according to VDZ

Parameter	Primary gas	Secondary gas
CO_2	35 vol.%	62 – 74 vol.%
O_2	up to 65 vol.%	18 – 23 vol.%
N_2	rest	8 – 12 vol.%
Ar	< 1 % vol.%	< 1.5 vol.%
H_2O	0 vol.%	1 – 2 vol.%
Temperature	30 - 50 °C	700 – 1100 °C
Velocity	15 – 20 (max.40) m/s	at the burner tip 5 -10 (max 15) m/s

- Primary gas rate: 10 -15 %
- Flame length ~ 1/3 kiln length

2.2 Downscaling criteria and constraints

Downscaling of industrial size machinery requires a trade-off between prototype scaling factor, process requirements/constraints and desired machinery size on the one hand and technical constraints like manufacturability of single machinery parts, reuse and adaptability of existing test rig / trial facility on the other hand.

This project has received funding from the European Union's Horizon2020 Research and Innovation Programme under Grant Agreement No 641185

In this case, several requirements limited the size of the prototype burner, resulting in an imprecise quantitative transfer function of pilot scale testing results to industrial size. The major constraints influencing the burner design were:

- The maximum thermal test rig size is 500 kW, the limitation of the burner combustion capacity is caused by the existing exhaust gas system. Referring to the BAT plant in [1] producing 3000 tpd clinker with a thermal heat consumption of 3026 kJ/$kg_{clinker}$ and a share of 45% of the thermal energy required in the sintering zone, the sintering zone burner would be designed for a thermal capacity of 47 MW under operating conditions (Scaling factor of approximately 100).
- The secondary gas temperature is limited to 800 °C this restriction is caused by the design of the electrically operated gas preheaters. An impact on fuel reaction velocity (longer flame, softer flame, etc.) is expected.
- The inner diameter of the combustion chamber is fixed to 800 mm, resulting in low secondary air and exhaust gas speeds compared to an industrial kiln.
- The primary gas flow rate (nozzle gas amount) is defined by minimum manufacturable nozzle diameter (5 mm), the number of nozzles (8x) and the design figure for the nozzle exit gas velocity (250 m/s).
- The fuel transport gas flow rate is defined by the minimum annular gap size of the channel. For manufacturing reasons the annular gap was set to 3.2 mm, the design figure for the transport velocity is 15 m/s.

The scaling factor of nearly 100 (or two magnitudes) between industrial and pilot application was considered to be a reasonable stepping size regarding the design of pyroprocessing equipment for cement plant applications.

The number of nozzles inside the burner was determined by a design number, which is applied to industrial sintering zone burners. Table 2.3 and Figure 2.1 compare burner and kiln diameter for the final design. The ratio of furnace to burner diameter is two times higher in the pilot testing compared to typical industrial scenario. This difference is expected to affect the secondary gas flow pattern in the region close to the burner or even secondary gas entrainment.

Table 2-3: Size ratio comparison of burner and kiln diameter

Case	Kiln diameter / burner diameter
Downscaled burner	10.66
Industry	5

This project has received funding from the European Union's Horizon2020 Research and Innovation Programme under Grant Agreement No 641185

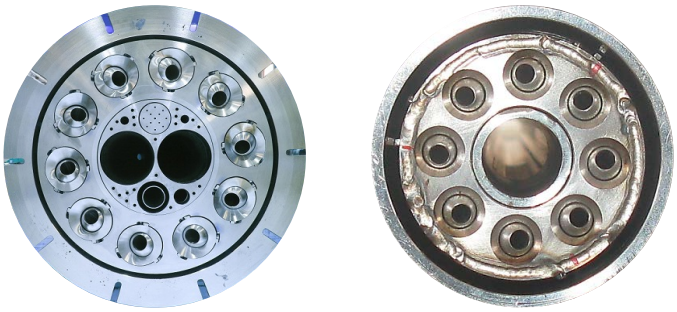

a) b)

Figure 2-1: Comparison burner tip of: a) real scale and b) downscale burner.

2.3 Prototype burner design

Figure 2.2 shows the main components of the burner assembly. Inlets for coal and carrier gas, as well as primary gas are indicated. The primary gas is supplied as premixed pressurized gas and exits through the nozzles at the burner tip.

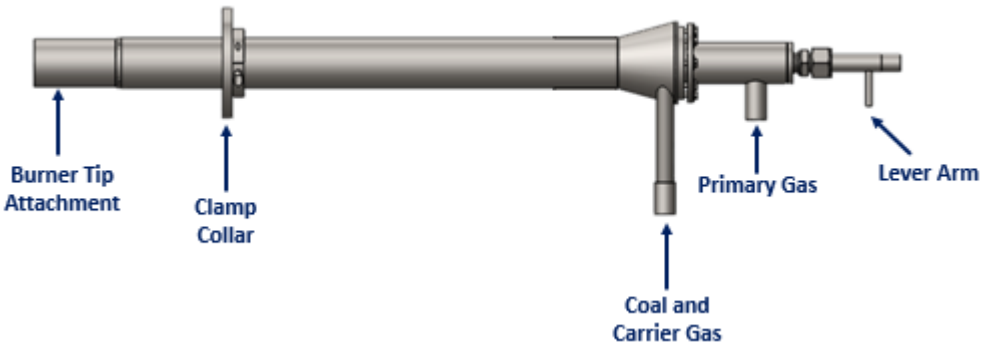

Figure 2-2: Burner assembly.

Figure 2.3 shows the tip of the downscaled burner including details of the swirl generator. The inner pipe along with the outer pipe and the swirl generator form a 3.25 mm annular gap for solid fuel and carrier gas. The fuel exits with a speed of approximately 15 m/s. The axial position of the burner is adjustable by a clamp collar up to 500 mm inside the combustion chamber.

In the swirl generator, the primary gas exits with high momentum via 8 nozzles of inner diameter 5 mm. The nominal swirl angle is adjustable from 0° to 40° by a rotating shaft and disc mechanism, which is manually actuated using a lever arm (cf. Figure 2.2 and 2.3). The rotating shaft also serves as means to introduce gas for ignition. The burner has an outer diameter of 75 mm and a total length of 1114 mm.

This project has received funding from the European Union's Horizon2020 Research and Innovation Programme under Grant Agreement No 641185

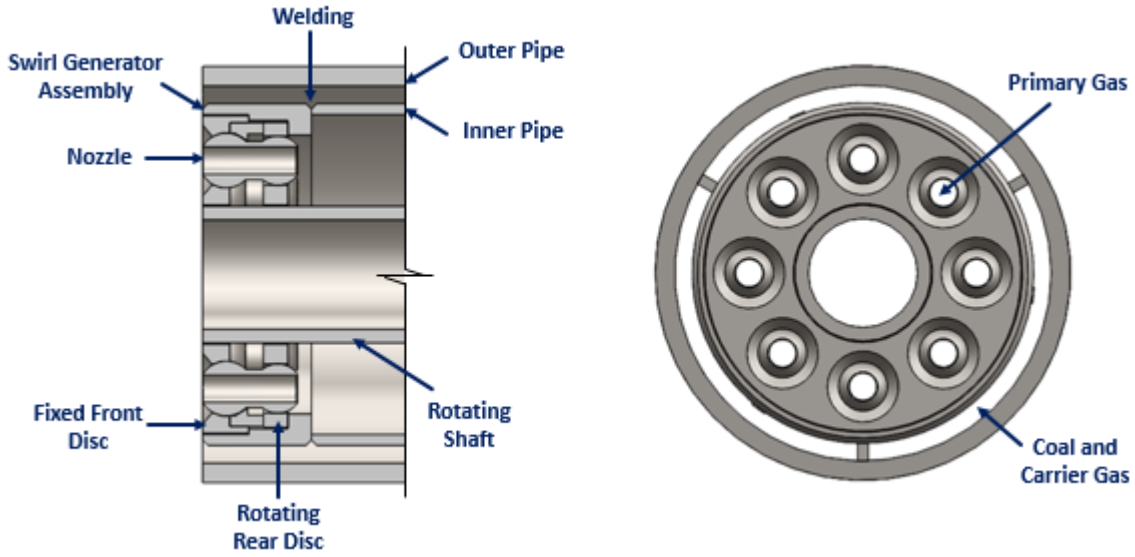

Figure 2-3: View of burner tip attachment

In Figure 2-4 a view of the burner mounted in the pulverized coal combustion chamber of IFK is shown. Unlike the case of a cement kiln, the burner was installed overhead in the combustion chamber. The combustion chamber has an inner diameter of 800 mm and is lined with refractory. The burner was engineered by TKIS and manufactured by IFK, other equipment like primary, secondary and transport gas supply system, preheating system for secondary air, combustible supply system, IR flame detectors, gas ducts and exhaust gas treatment system were already present or engineered by IFK.

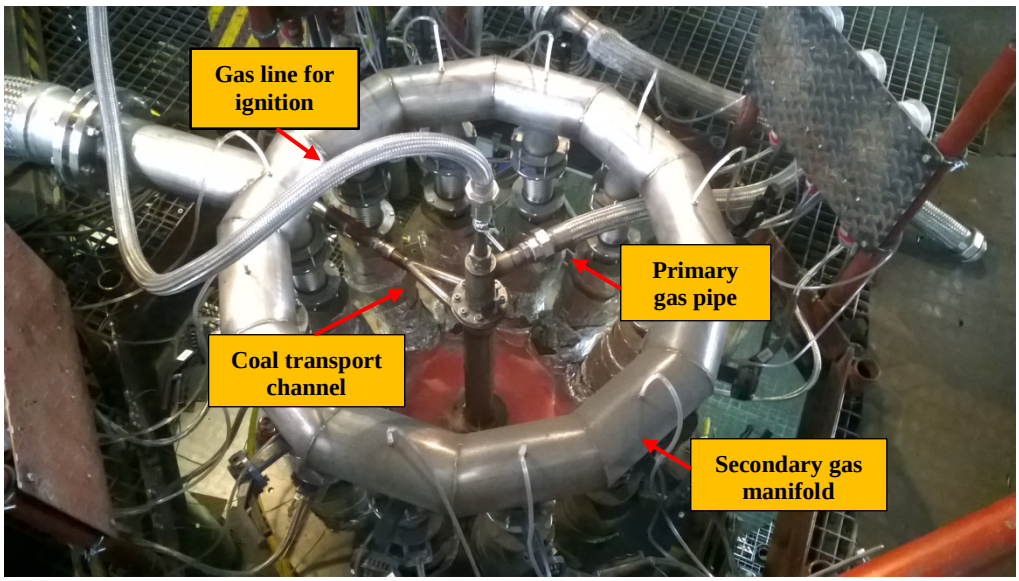

Figure 2-4: Burner mounted on top of the combustion chamber during demonstration tests. Surrounding the burner a circular manifold for secondary gas distribution.

This project has received funding from the European Union's Horizon2020 Research and Innovation Programme under Grant Agreement No 641185

2.4 Burner modifications

The original engineering design from TKIS was slightly modified to ease the manufacturing and future repair of the nozzle section. The sections modified were the diameter of the primary gas and fuel transport pipes. However, the first 150 mm pipe section of the burner was not modified and remains according to the original design, in that way the calculated gas velocities were not affected. An advantage of the re-design is an increased flexibility in case of damage in the burner tip section. Since the burner tip is exposed to elevated temperature and mechanical stresses the possibility of damage is increased together with the theoretical need to replace nozzles, etc. As shown in Figure 2-5, the first section of the burner was redesigned to be modular and is assembled with the rest of the burner body through a pipe thread.

Figure 2-5: Flexibility by unmounting nozzle section in modified design.

This project has received funding from the European Union's Horizon2020 Research and Innovation Programme under Grant Agreement No 641185

3 DEMONSTRATION TESTS SETUP

3.1 Facility description

The combustion chamber of the 500 kW top-fired furnace (see Figure 3-1) has a total length of 7 m and an inner diameter of 0.8 m. Refractory lining covers the inner surface of the upper four meters of the combustion chamber. The furnace is equipped with multiple measurement ports distributed along the length of the reactor where specialized probes are introduced to perform in-flame measurements. One gas analyzer monitors on a continuous basis concentration of the exit gases main components while data is recorded for later analysis. A second gas analyzer serves as an axial/radial gas monitor due to the flexibility to move the sampling point from port to port, giving the possibility to create an axial and radial gas profile inside the reactor.

Additional equipment is located along the flue gas cleaning train with the option to remove gas pollutants (SCR, dust electro-filter, bag filter). The recirculation of exhaust gases back to the furnace is possible, however, during the tests reported here a synthetic recirculation, i.e. a controlled mixture of CO_2 and O_2 from storage tanks was used. The justification for this decision lays in the need to avoid a wet recirculation with the additional advantage that a better control of primary, carrier and secondary gas composition was achieved in this way.

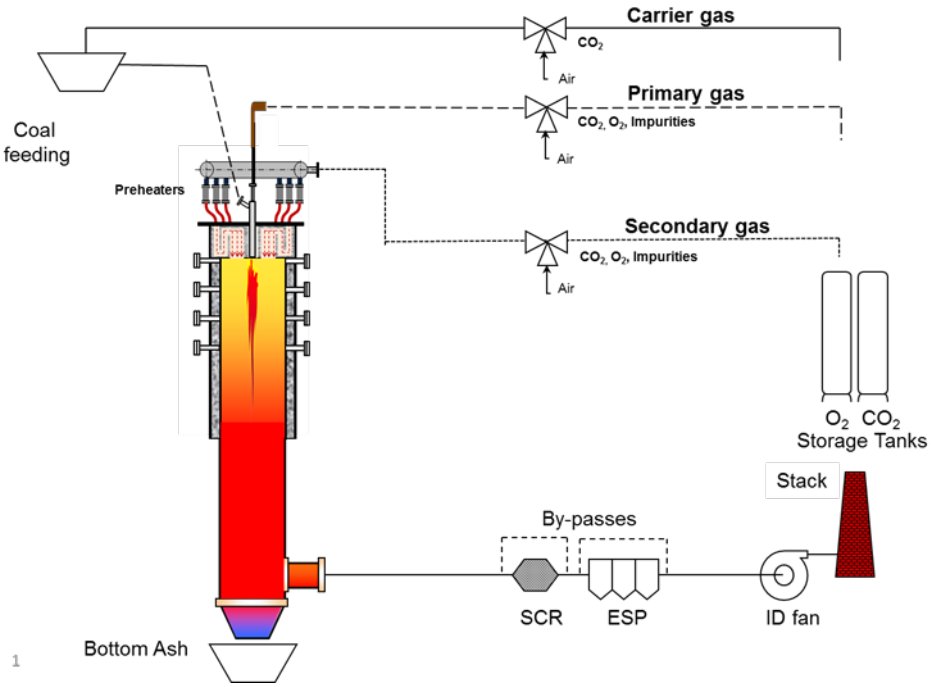

Figure 3-1: KSVA 500kW$_{th}$ test facility

The facility was adapted for these tests by installing an electrical preheater system to allow the preheating of the synthetic recirculation (secondary gas) up to 800 °C simulating the flue gas recirculation of an oxy-fuel cement kiln after preheating in the clinker cooler. Figure 3-2 shows a sketch of the secondary gas preheater system installed in the furnace ceiling surrounding the burner. The secondary gas is distributed to the individual preheaters, each one with a capacity of 15 kW$_{el}$, by means of a circular manifold. The preheated gas is injected directly to the combustion chamber in an inner ring that surrounds the burner as it happens in cement kilns.

This project has received funding from the European Union's Horizon2020 Research and Innovation Programme under Grant Agreement No 641185

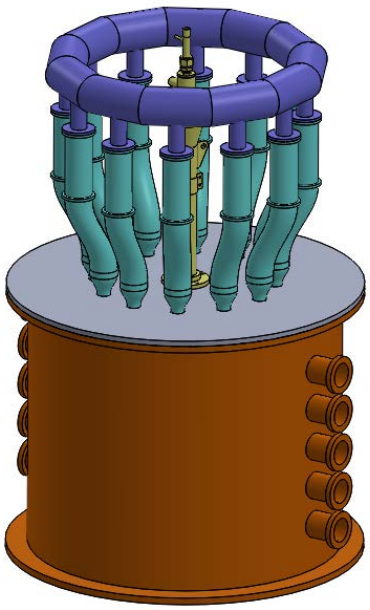

Figure 3-2: Sketch of the gas preheating circuit mounted on top of the furnace.

3.2 Experimental matrix

After corresponding commissioning of the preheater system and prototype burner, diverse demonstration tests were carried out to evaluate burner performance. Two fuels were used during the tests: predried lignite (reference fuel) and petcoke. Petcoke is a recovered solid fuel obtained from oil refineries. Both fuels are used extensively in cement plants around the world. Table 3.1 depicts the different test cases as well as measurements performed with each fuel. The nomenclature OF*XX* is an indication of the volume percentage of oxygen in the sum of primary, secondary and carrier gas. This value is inversely proportional to the recycle ratio in oxyfuel systems.

Table 3-1: Description of tests and measurements

	Tests with Petcoke	**Tests with Lignite**
Test Cases	Air, OF27, OF32	Air, OF9, OF32
Continuous measurements	O_2, CO_2, CO, NOx, SO_2 in furnace outlet	O_2, CO_2, CO, NOx, SO_2 in furnace outlet
Inflame measurements to create axial and radial profiles	O_2, CO_2, CO, NOx, SO_2 Gas Temperature	O_2, CO_2, CO, NOx, SO_2 Gas Temperature
Measurements at furnace wall	Total heat fluxes Radiative heat fluxes	Total heat fluxes Radiative heat fluxes
Additional investigations	Fuel burnout Primary gas flow variation Carrier gas flow variation Burner location	Fuel burnout Swirl variation Oxygen enrichment in primary gas

This project has received funding from the European Union's Horizon2020 Research and Innovation Programme under Grant Agreement No 641185

3.3 Fuel characterization

As can be observed from Table 3.2, petcoke is characterized for its higher carbon content and lower volatiles proportion compared to lignite. As a result, weaker ignition and less stable combustion was expected and later confirmed during the burner tests. Higher proportion of sulfur is found in petcoke, which explains the sticky behavior of deposits in reactor walls and outlet.

Table 3-2:Fuel analysis (an=as analyzed, wf=water free)

	Petcoke		**Lignite**	
	an	wf	an	wf
NCV [MJ/kg]	32,237	33,894	22,200	24,860
Water [%]	4,56	-	10,7	-
Ash [%]	2,12	2,22	3,02	3,38
Volatiles [%]	11,3	11,9	46,6	52,1
Cfix [%]	82,0	85,9	39,7	44,5
C [%]	77,0	80,7	58,4	65,4
H [%]	3,40	3,56	4,25	4,76
N [%]	1,47	1,57	0,702	0,786
S [%]	3,03	3,17	0,317	0,355

Both fuels were received in a milled and pre-dried state. Table 3.3 and Figure 3-3 show that in terms of particle size distribution both fuel were comparable.

Table 3-3: Characterization of particle distribution

	Petcoke	**Lignite**
D10	6 µm	6 µm
D50	33 µm	30 µm
D90	121 µm	150 µm

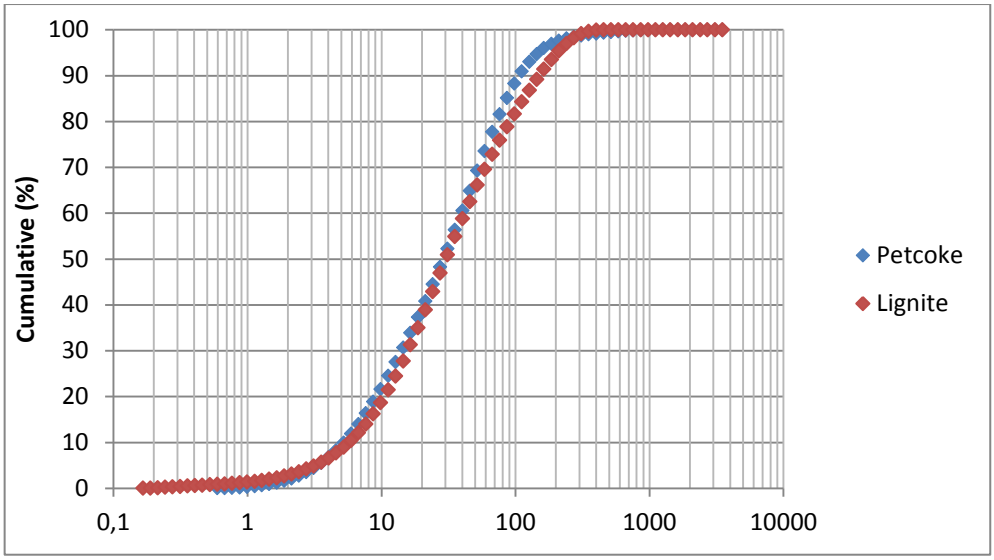

Figure 3-3: Particle Distribution

This project has received funding from the European Union's Horizon2020 Research and Innovation Programme under Grant Agreement No 641185

3.4 Inflow conditions

The results presented in this document are the product of several demonstration tests. In total three test cases were set for each fuel: two oxyfuel configurations and one reference air case. Table 3.4 and Table 3.5 contain details on the composition of main gas streams. The distribution of gases was set in accordance to the values proposed in Table 2.2 for oxyfuel operation. As observed in the tables below, similar air to fuel ratio was used to make the settings comparable.

During all tests the secondary gas was heated to 750 °C before entering the combustion chamber and otherwise stated the burner swirl angle was set to 20°.

Table 3-4: Inflow conditions in demonstration tests with petcoke

		Air	**OF27**	**OF32***
Thermal Input	kW	482	478	482
Primary gas composition	Vol.-%, wet	Air	53% O_2	70% O_2
			47% CO_2	30% CO_2
Secondary gas composition	Vol.-%, wet	Air	21% O_2	28% O_2
			79% CO_2	72% CO_2
Fuel carrier gas composition	Vol.-%, wet	Air	100% CO_2	100% CO_2
λ (air to fuel ratio)	-	1,09	1,13	1,09
Flame momentum	% m/s	1777	3607	2122

*For this test case only wall radiation and measurements at furnace outlet are available.

Table 3-5: Inflow conditions in demonstration tests with pre-dried lignite

		Air	**OF29**	**OF32**
Thermal Input	kW	400	400	400
Primary gas composition	Vol.-%, wet	Air	60% O_2	60% O_2
			40% CO_2	40% CO_2
Secondary gas composition	Vol.-%, wet	Air	19,5% O_2	23,5% O_2
			80,5% CO_2	76,5% CO_2
Fuel carrier gas composition	Vol.-%, wet	Air	100% CO_2	100% CO_2
λ (air to fuel ratio)	-	1,10	1,10	1,10
Flame momentum	% m/s	2688	4775	5411

This project has received funding from the European Union's Horizon2020 Research and Innovation Programme under Grant Agreement No 641185

3.5 Flame momentum

In conventional cement furnaces, primary air is injected through the burner with high momentum in order to promote hot secondary gas entrainment. Adequate secondary gas entrainment leads to improved mixing, ignition and the formation of an intense radiating flame. Flame momentum or flame impulse is calculated by multiplying the percentage of primary gas (volume percentage in relation to total inlet gases) times the primary gas velocity. *Table 3.6* shows typical values of flame momentum for typical coals and petcoke. The higher the momentum, the better the entrainment of secondary air and the faster the combustion of fuel. However, momentum obtained by low primary air % and higher velocity is better than higher primary air % and lower velocity. The latter because lower velocity negatively affects secondary gas entrainment and also because a high share of primary gas cools the flame (primary gas is not preheated). Aiming to keep high primary gas velocity, the percentage of primary gas during the experiments was kept in the range of 20-35%, which was higher than typical values found in *Table 2.1* while the primary gas velocity was in the range of 110-160 m/s. Though high flame momentum was obtained (see values in Table 3.4 and Table 3.5), secondary gas entrainment and flame temperature were expected to be affected.

Table 3-6: Typical flame momentum in modern cement burners

Fuel	Flame momentum = % primary gas * velocity of primary gas
Typical coal	1200 – 1500 % m/s
Petcoke	>2500 % m/s

This project has received funding from the European Union's Horizon2020 Research and Innovation Programme under Grant Agreement No 641185

4 RESULTS

The burner design was evaluated in terms of the suitability to operate under CO_2/O_2 conditions and produce similar combustion behavior as in combustion with air. In addition to investigate combustion behavior, fuel flexibility was also targeted. As mentioned in section 3.2, two conventional fuels were selected: predried lignite and petroleum coke (further referred as petcoke). Both fuels are used in many cement plants and cover a good spectrum of fossil fuels usage. The selection of these fuels aims to show the differences in firing low volatile and high volatile fuels. As a complementary result several parameters including primary gas composition and swirling angle were varied in order to assess their influence in shaping temperature, radiation and gaseous emissions profiles. Milestone 7.6 includes a detailed account of measured data for reference.

4.1 Combustion performance

Oxygen consumption can be seen as an indicator fuel consumption progress and ignition behavior. Figure 4-1 shows the oxygen concentration measured at the centerline in air and oxyfuel conditions during the experiments with both fuels. It is observed that oxygen consumption rate was faster by firing lignite compared to petcoke. While stoichiometric oxygen in air combustion is consumed after 3 m in petcoke combustion (Figure 4-1, left figure), it only needs a trajectory of one meter to be consumed when using lignite (right figure). This behavior is explained by the low proportion of volatiles and large proportion of fixed carbon in petcoke (see Table 3.2). Volatile components are oxidized faster than char, which explains the faster consumption of oxygen in lignite combustion. In order to obtain faster combustion of petcoke particles improved burning conditions are necessary, including higher secondary gas temperature and burner momentum.

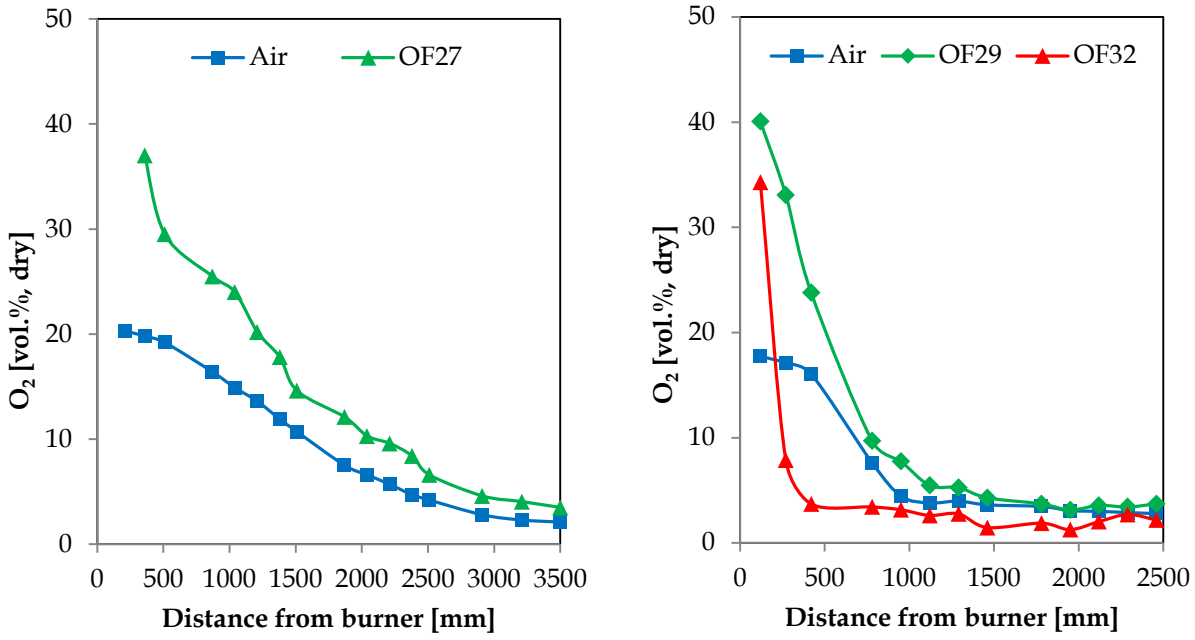

Figure 4-1: Oxygen consumption along the furnace centerline. Left: petcoke, Right: lignite.

This project has received funding from the European Union's Horizon2020 Research and Innovation Programme under Grant Agreement No 641185

The rate of oxygen consumption, meaning the required distance to consume stoichiometric amount of oxidizer, between oxyfuel and air combustion was found to be similar for OF27 (petcoke) and OF29 (lignite). In these two oxyfuel cases oxygen concentration is higher in the burner vicinity resulting from a high proportion of oxidizer in the primary gas outlet, its consumption is finished at similar distance compared to the reference air case. The OF32 lignite case shows faster oxygen consumption possibly explained by higher energy release in the burner vicinity region.

Carbon dioxide is the main product of combustion. Under oxyfuel conditions with dry recirculation (no water vapor in inlet gases), the calculated CO_2 composition in combustion products is expected to rise close to 95 vol.% in dry condition. As seen in Figure 4-2-left, during petcoke oxy-combustion the carbon dioxide composition keeps significantly low even at 3.5 distance from burner outlet. However, the value registered by the gas analyzer close to the furnace outlet (5 meters from burner) was 85 vol.% dry. This last information evinces that longer residence time was needed to fully complete the combustion of petcoke particles. Also, a second factor that could influence this result was undesired air entrance to the reactor. Figure 4-2-right shows that under lignite combustion the production of CO_2 reaches a value close to 90 vol.%, The red line evinces that by increasing oxidant proportion (OF32), the reaction proceeds faster.

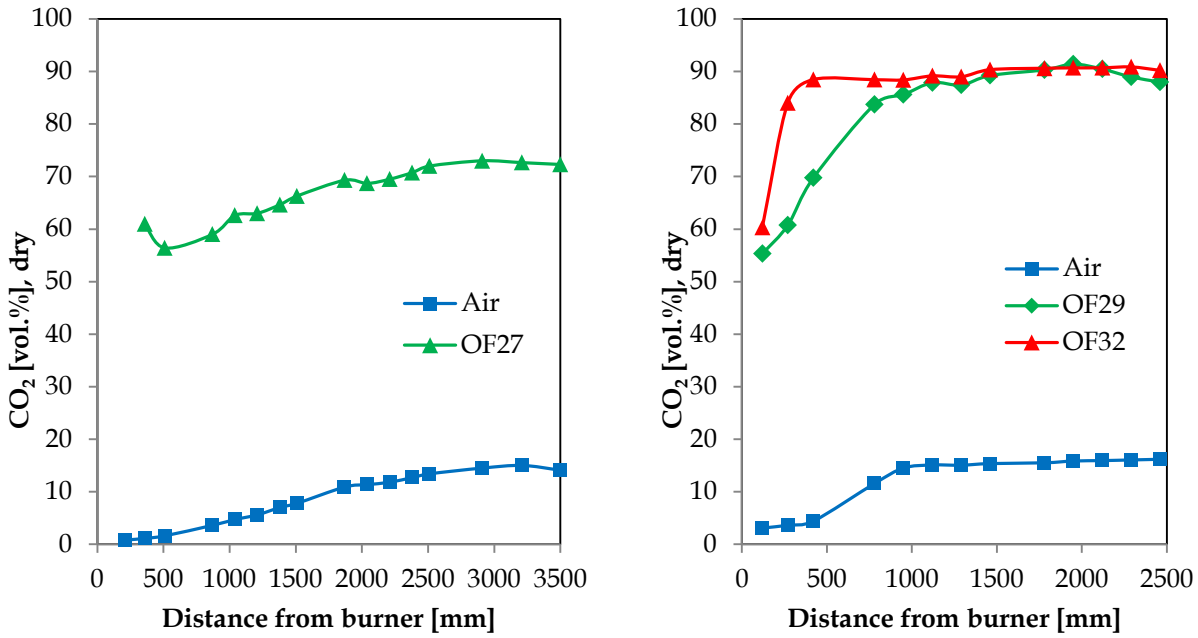

Figure 4-2: CO_2 production along the furnace centerline. Left: petcoke, Right: lignite.

Carbon monoxide is an indicator of incomplete combustion. Its formation is influenced by several factors including: fuel type, furnace temperature, ambient composition, among others. As observed in Figure 4-3 CO emissions registered during lignite combustion were significantly higher compared to demonstration tests with petcoke (consider differences in y-axis range). This behavior is attributed to the difference in volatile content of these two fuels. Hydrocarbons from volatile components react faster to produce CO, compared to the time scale needed to fully

This project has received funding from the European Union's Horizon2020 Research and Innovation Programme under Grant Agreement No 641185

convert CO to CO_2, which favors high CO peaks in the flame region. This phenomenon is more visible during combustion of high volatile fuels like lignite.

On the other side CO emissions are higher in O_2/CO_2 conditions compared to air firing. This may be attributed to the heterogeneous gasification reaction (Bouduard reaction) where char reacts with abundant CO_2 to produce two molecules of CO ($C_{(s)} + CO_2 \leftrightarrow 2CO$). This reaction is endothermic in the CO direction and therefore, favored at high temperatures, which would also explain why OF32 produced significantly higher CO values compared to OF29 (see Figure 4-3-right).

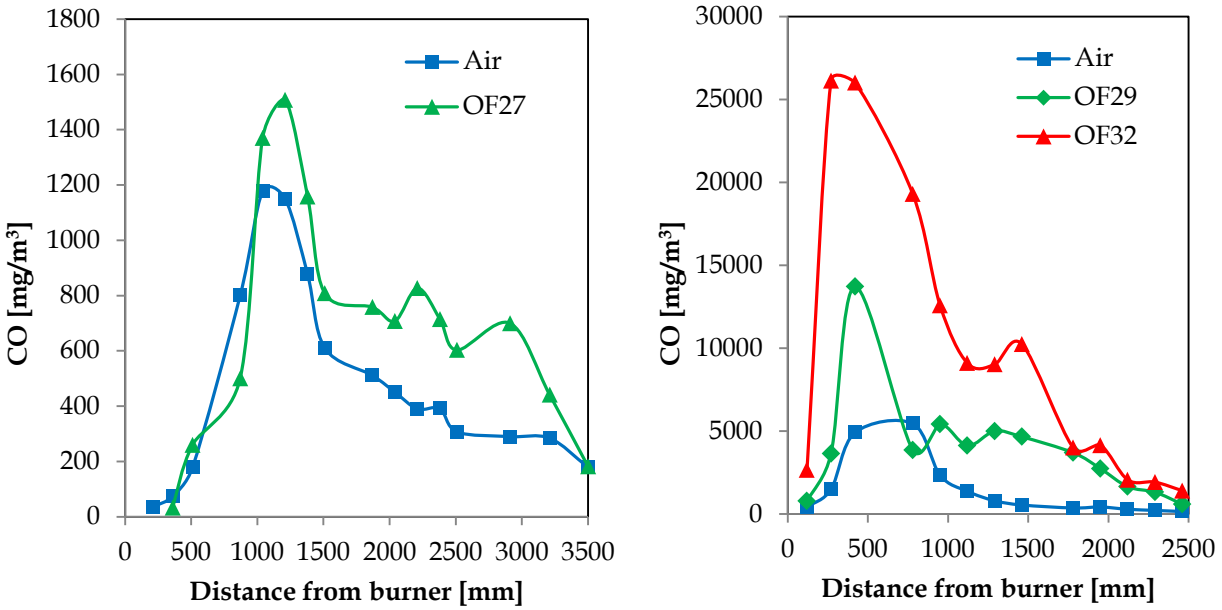

Figure 4-3: CO production along the furnace centerline. Left: petcoke, Right: lignite.

4.2 Pollutants formation

4.2.1 Nitric oxides (NO_x)

One of the major goals of oxyfuel combustion is to avoid the formation of nitrogen oxides, which complicate CO_2 purification in further post-processing units. Although air, the main source of nitrogen, is restricted during oxyfuel conditions, significant amounts of nitrogen may still be injected to the furnace through fuel-bounded nitrogen and small air leakages. Figure 4-4-left shows the time averaged measured dry composition of nitrogen oxides along the centerline of the furnace. The proportion of NO_x formed under air conditions is considerably lower than the values measured for both oxyfuel cases. This behavior is not surprising considering that the main formation-mechanism of NO_x is temperature dependent. Beside from higher NO_x proportion, faster formation is observed by increasing oxygen enrichment in inlet gases.

Although NO_x measurements were clearly higher in oxy-firing condition, it should be remembered that these experiments were conducted without a real recirculation circuit

This project has received funding from the European Union's Horizon2020 Research and Innovation Programme under Grant Agreement No 641185

(secondary gas was injected from storage tanks). It has been demonstrated that 50-80% of NO produced in oxyfuel systems can be reduced to N_2 when recycled back to the furnace [2]–[4]. Moreover, the flue gas volume flow from oxy-firing systems is reduced up to 80% depending on the recirculating ratio applied. Figure 4-4-right compares the NOx emissions considering the equivalent recirculation ratio of tested oxyfuel cases (OF29 ≈ 60%, OF32 ≈ 57%). By increasing the recirculation ratio, less volume flow is emitted. The values in Figure 4-4-right are expressed in mass per energy input to account for these volume flow differences. In general terms the emission per unit of fuel energy supplied is reduced to about 50% for oxyfuel cases compared to air-fired conditions.

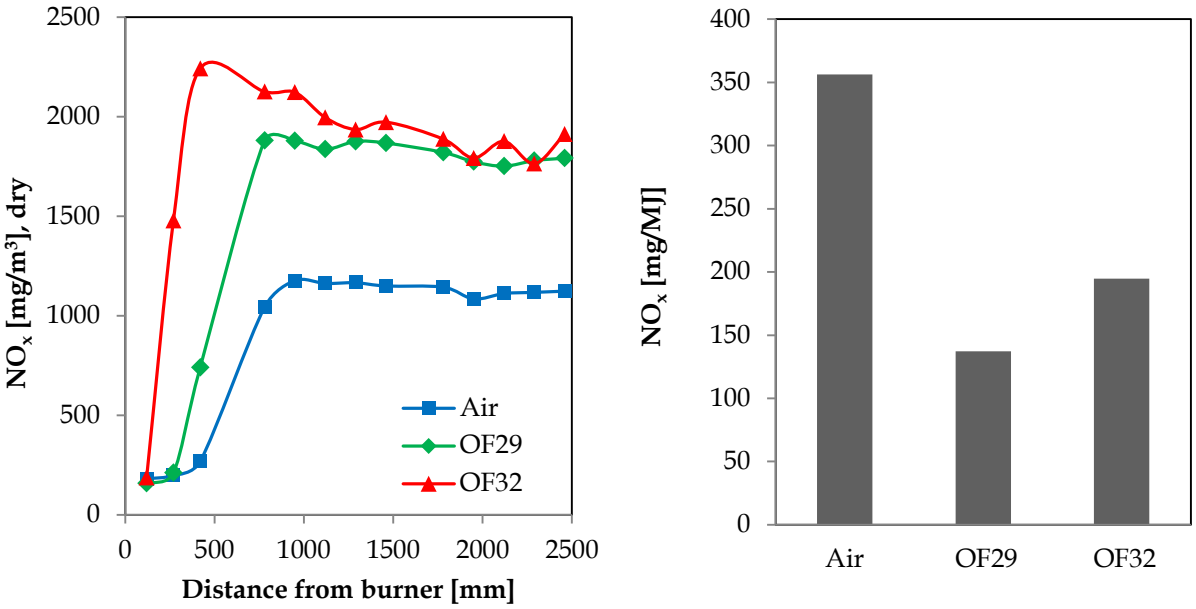

Figure 4-4: Measurements of NOx along the centerline of the furnace (left). NOx emissions considering flue gas reduction (right).

In summary, higher NO_x concentrations were observed in oxyfuel mode compared to air. Moreover, NO_x was also seen to increase with elevated oxygen enrichment. However, when considering flue gas reduction, emissions of this pollutant are lower in terms of mass per energy input. A better assessment of NO_x reduction mechanism could be carried out with additional testing including flue gas recycling.

4.2.2 Sulfur dioxide (SO_2)

Higher concentrations of SO_2 were also observed during oxyfuel firing compared to combustion in air conditions. As pictured in Figure 4-5-left, the concentration of SO_2 during OF32 resulted almost four times higher than air values, while the values measured for OF29 resulted close to two times higher. As evinced, the oxidation of sulfur benefits from higher oxygen availability in oxyfuel mode. Similar to NOx emissions, this result is put in perspective when considering the reduction in flue gas volume. Figure 4-5 presents the values measured at furnace outlet re-

This project has received funding from the European Union's Horizon2020 Research and Innovation Programme under Grant Agreement No 641185

calculated in mass over energy input. The SO_2 emissions in OF29 are close to 50% lower than in air combustion while in OF32 the value is similar to air combustion. This result could be incremented by the effect of sulfur accumulation in systems with flue gas recycle.
However, in a real cement kiln sulfur emissions are expected to be reduced due to an inherent capture of sulfur by the raw material in the cement kilns and calciner. Sulfur dioxide reacts with the material feedstock to form sulfates which participate in the formation of cement clinker.

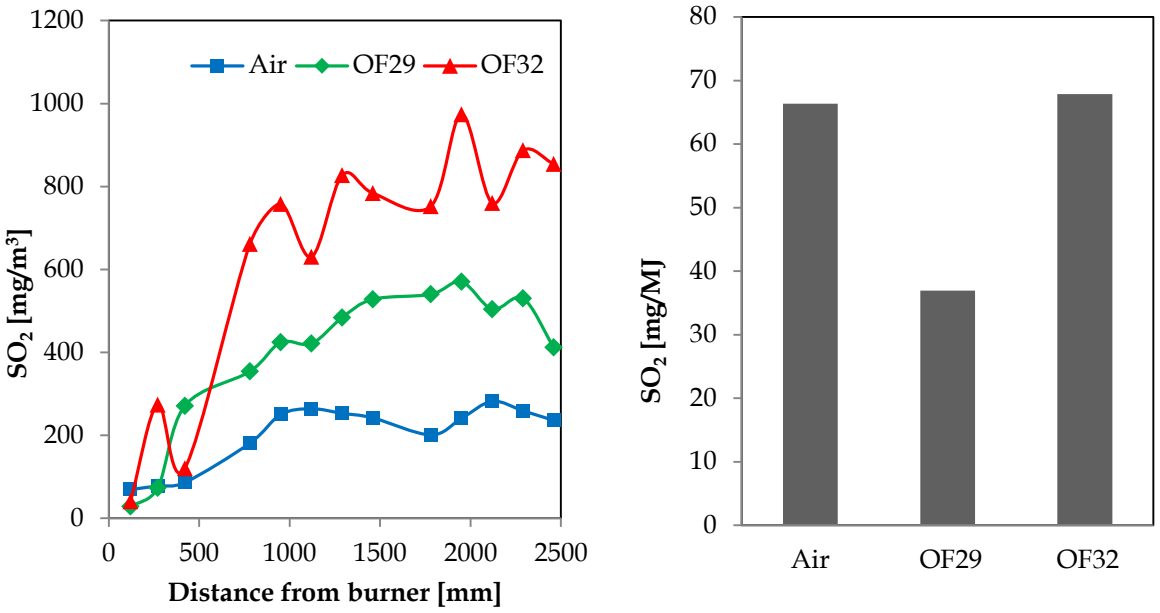

Figure 4-5: Measurements of NOx along the centerline of the furnace (left). NOx emissions considering flue gas reduction (right).

4.3 Gas temperature profiles

Flame temperature is influenced by the combustion atmosphere. Due to higher heat capacity of carbon dioxide molecules compared to nitrogen, lower flame temperature is expected in O_2/CO_2 systems compared to O_2/N_2 for comparable volume proportion of oxygen. For this reason oxyfuel systems typically work with enriched oxygen conditions higher than 21 vol.% to obtain temperature levels comparable to air combustion.

Gas temperature was measured with a Type B thermocouple mounted in a water cooled probe. Figure 4-6-left compares the temperature profile measured under air and OF27 during combustion with petcoke. It can be observed that similar peak temperature was obtained for both systems. However, OF27´s peak was shifted one meter downstream probably due to slower kinetics. During lignite combustion, the highest temperature peak is measured closer to the burner tip compared to petcoke (see Figure 4-6-right). Besides, a higher temperature profile is achieved when increasing the oxygen proportion higher than 29 vol.%. In both figures far from the burner region the temperature distribution becomes more similar to each other. During lignite combustion (right) it is also observed that the peak of maximum temperature is shifted towards the burner as the oxygen proportion is increased. This earlier energy release is an indicator of faster kinetics, favored by more abundant oxidizer.

This project has received funding from the European Union's Horizon2020 Research and Innovation Programme under Grant Agreement No 641185

A similar result is observed for the gas temperature at the position close to the wall. As observed in Figure 4-7, the closes air-like temperature profile is obtained with the OF27 mode, while slightly higher temperature is measured if oxygen proportion is increased to OF29.

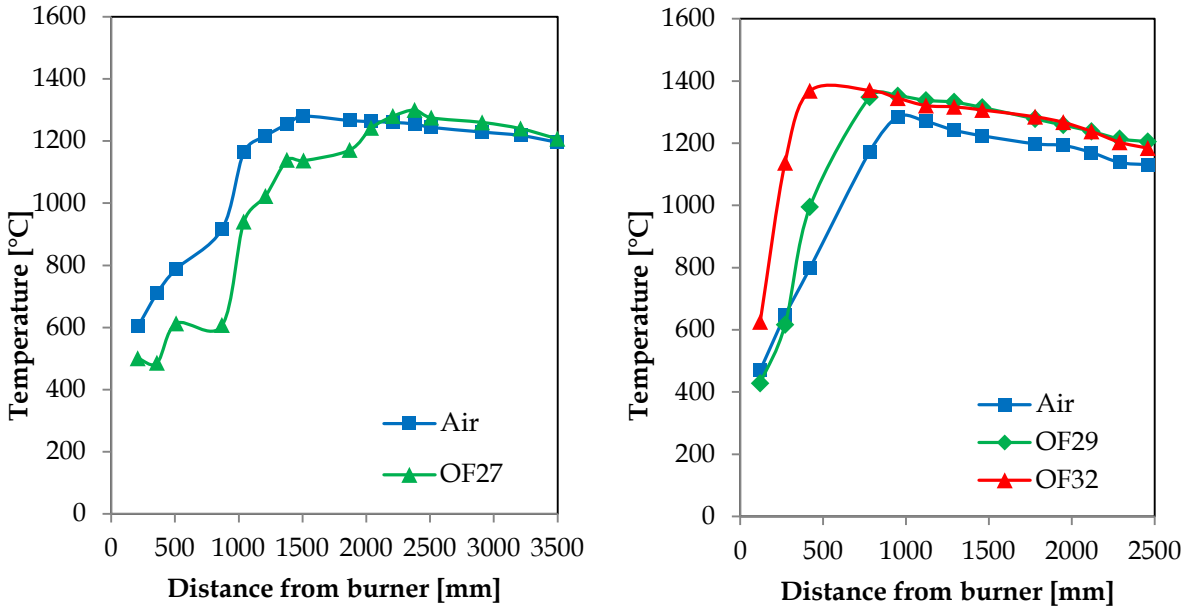

Figure 4-6: Gas temperature along the furnace centerline. Left: petcoke, Right: lignite.

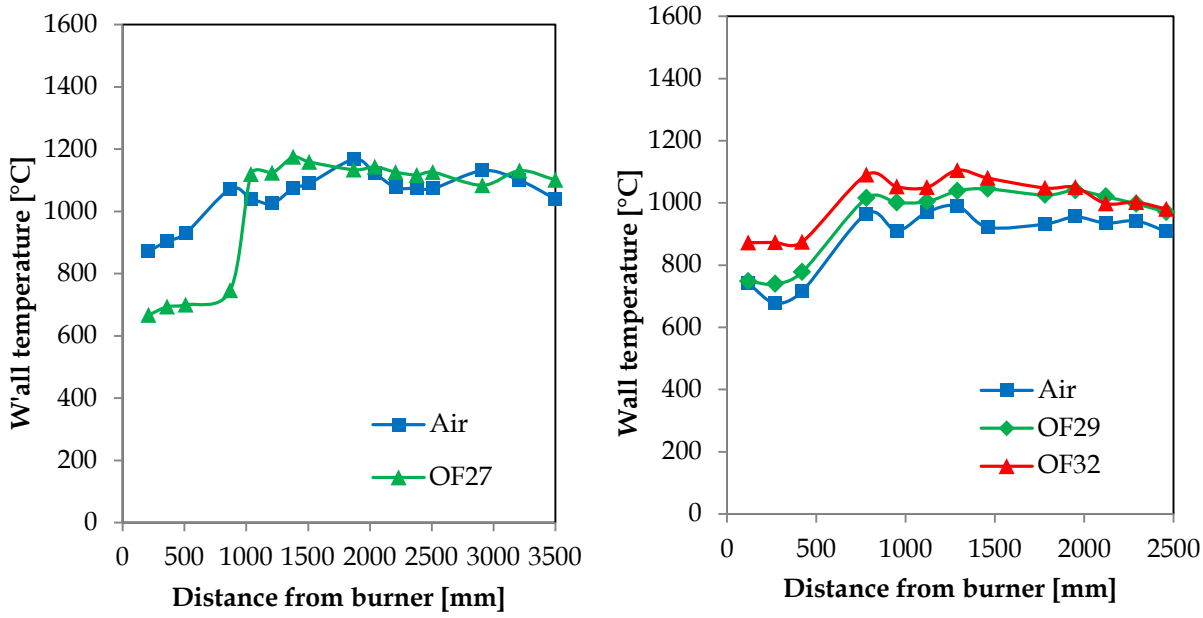

Figure 4-7: Gas temperature measured close to furnace wall. Left: petcoke, Right: lignite.

The air and OF29 cases during lignite combustion where compared more in detailed by interpolation of 70 radial and axial measurements of gas temperature in Figure 4-8. As observed, similar ignition and temperature distribution was found between the two cases.

This project has received funding from the European Union's Horizon2020 Research and Innovation Programme under Grant Agreement No 641185

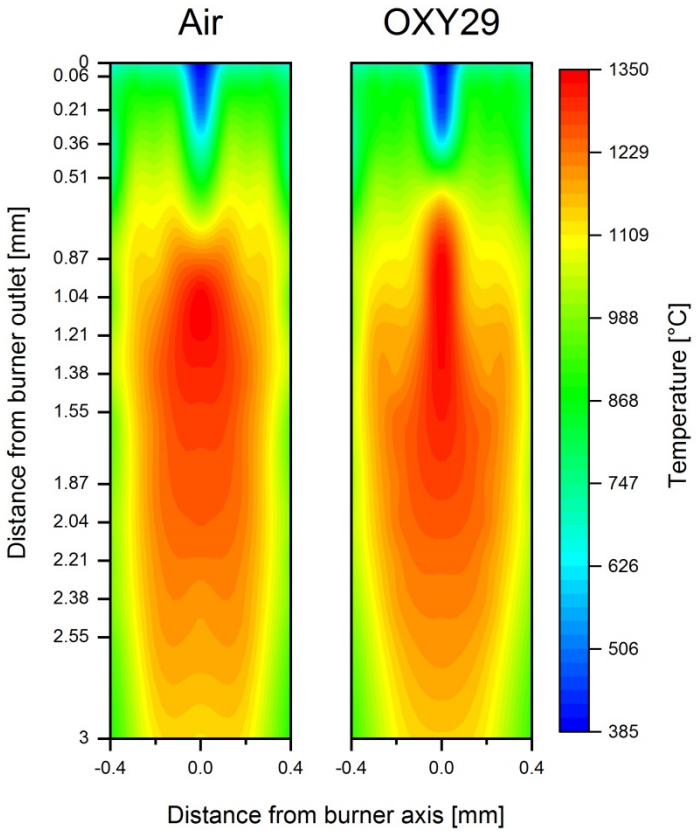

Figure 4-8: Gas temperature distribution in air and OF29 cases during lignite combustion.

Maximum temperatures obtained in both air and oxyfuel cases were in the range of 1350-1400 °C, which for cement production conditions appear to be too low. In industrial cement kilns flame temperature may be as high as 1800 °C. A sufficient gradient of temperature is important to enable heat transfer between combustion gas and material. The registered lower temperature peaks during the experiments may be explained by the proportion of heat losses/air entrance that in a pilot facility may be higher compared to the industrial application. Furthermore, due to downscaling limitations previously explained, the proportion of primary gas (at ambient temperature) was higher than in industrial scenario (~30% vs ~15%), which could have cooled the flame to a certain extent. Moreover, the secondary gas was nearly 700 °C (clearly lower than in cement kilns) and had a lower flow velocity (~1 m/s) what could have affected secondary gas entrainment creating a kind of staged combustion and may explain the quite flat profiles observed of temperature and heat fluxes.

4.4 Heat fluxes

Radiation is the main mechanism of heat transfer in cement kilns. Other mechanisms involved are conduction and convection. Differences in radiative heat transfer between oxyfuel and air combustion were expected due the radiant nature of the main components of oxyfuel flue gases. Carbon dioxide and water vapor absorb and emit radiation in the infrared spectrum while nitrogen, main component in air combustion, remains neutral to radiation. Additionally, flame temperature is expected to influence radiation intensity; the latter due to the strong non-linear

This project has received funding from the European Union's Horizon2020 Research and Innovation Programme under Grant Agreement No 641185

relation of radiation intensity with temperature as described by the Stefan-Boltzmann equation ($F = \sigma\varepsilon T^4$). Bodies with higher temperature radiate more.

Two types of heat fluxes were measured during the combustion tests. Incident heat radiation to furnace walls was measured with a MEDTHERM gardon gauge heat flux sensor mounted in a water cooled probe. The sensor itself was water cooled, which means that the measurements capture total radiation incident from the flame and entire reactor room to the sensor surface and don't account for the radiation that is reflected back. A quartz window was implemented to filter heat transfer by convection. Further, a small amount of nitrogen was used as purge to keep the optical view free from particle deposition. The probe has a wide angle of view and was calibrated in a black body furnace prior to the tests.

Total incident heat fluxes were also measured at furnace wall. The measurements account not only for incident radiation but also conduction and convection. The instrument used was a water-cooled Total Heat Flux Meter with a view angle of 180°.

Measurements were done at the furnace wall (400 mm from center line) at numerous axial distances from the burner tip to create an axial profile. As observed in the left plot in Figure 4-9, oxyfuel combustion with petcoke presented higher radiative heat flux to furnace wall compared to air combustion, with a difference in the range of 50 kW/m^2 beginning at the distance of 1000 mm until 3000 mm. This difference is mainly attributed to the high concentration of CO_2/H_2O since flame temperature was found to be similar in both scenarios (see Figure 4-6, left)

During lignite combustion (see Figure 4-9- right) both oxyfuel cases clearly presented higher radiative heat flux towards the wall than air combustion. This result can be a combination of the influence of high CO_2/H_2O concentration and the fact that both oxyfuel modes produced higher flame temperature than combustion with air (see Figure 4-6, right).

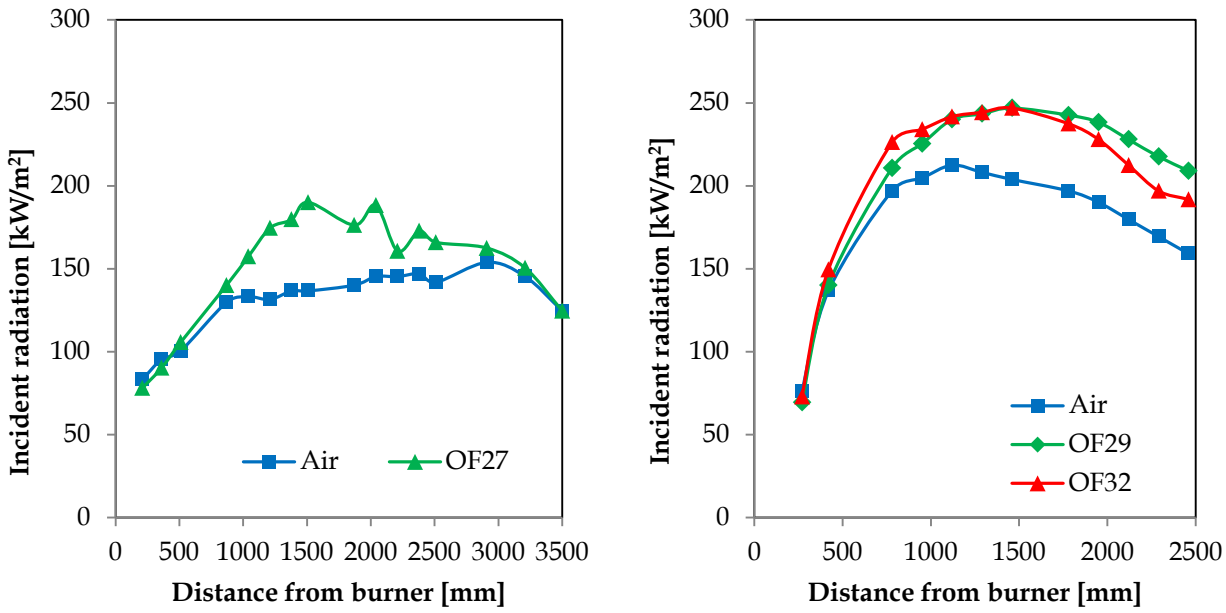

Figure 4-9: Axial radiative heat flux incident to the wall. Left: petcoke, Right: lignite.

This project has received funding from the European Union's Horizon2020 Research and Innovation Programme under Grant Agreement No 641185

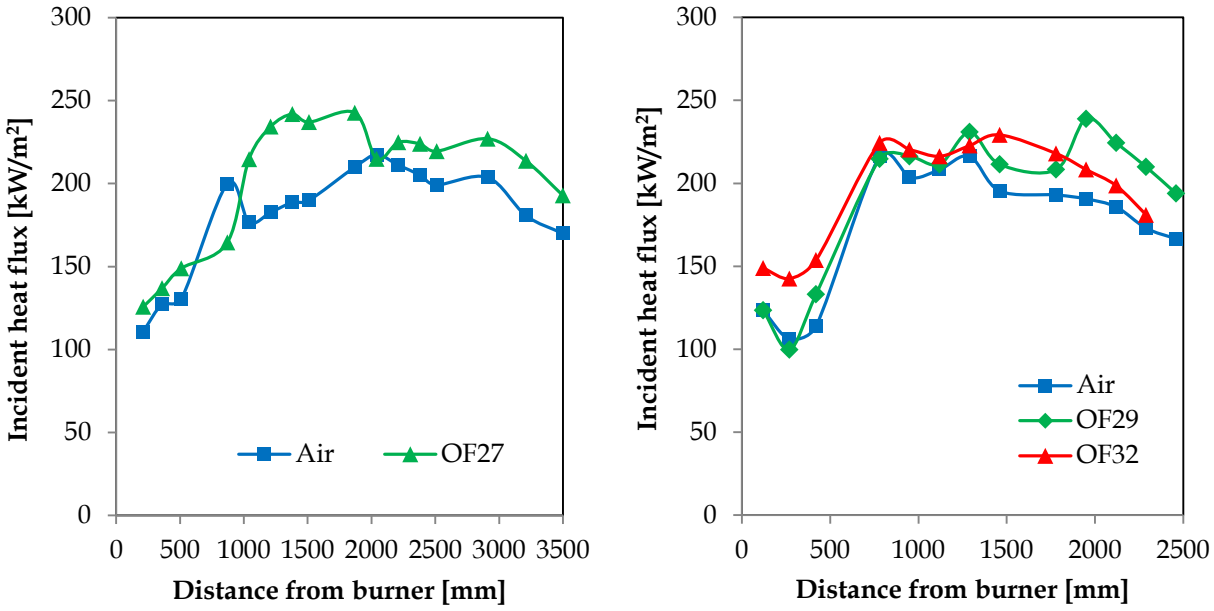

Figure 4-10: Axial total heat flux incident to the wall. Left: petcoke, Right: lignite.

The measured values of total heat flux, which also include convective and conductive heat transfer, are presented in Figure 4-10. As observed in the left figure, values recorded during petcoke combustion present the same trend as in Figure 4-9- left. Higher heat flux to the wall is measured by OF27. However, during lignite tests the difference in heat flux measured in oxyfuel mode and air combustion is reduced significantly. The values also oscillate avoiding a clear trend. These results indicate a strong influence of convective heat transfer creating turbulence in the near burner area. Heat transfer by convection is increased during lignite combustion considering that higher flame momentum was produced (see also Table 3.5).

In summary, higher radiation intensity to furnace walls is observed during oxyfuel combustion compared to air firing for the tested scenarios. Flame temperature is an influencing factor on radiation heat, as long as the flame temperature is higher during oxyfuel combustion, heat fluxes will also remain higher. From the present tests it can be deduced that an oxygen enrichment in total combustion gases slightly lower than 27 vol.% could produce lower radiation intensity than air firing.

4.5 Effect of oxygen enrichment in primary gas

As already explained, primary gas was injected through an arrangement of eight nozzles with movable swirl angle. The oxygen concentration in primary gas is an additional parameter to vary and was fixed during the first tests to 60% Vol. (resting 40% was CO_2). In a previous study by ECRA, CFD simulations were used to investigate flame formation and optimum burner operation in oxyfuel mode. It was observed that under oxyfuel conditions, the production of CO is significantly increased due to the influence of the Bouduard reaction ($C_{(s)} + CO_2 \leftrightarrow 2CO$), increasing flame length and affecting heat transfer from the gas to the material. As a result, it was suggested to increase oxygen content in the primary gas line to prevent undesired formation of CO. This suggestion was considered during test planning and is the reason why 60 Vol.% O_2 was used in the primary gas as a default value.

This project has received funding from the European Union's Horizon2020 Research and Innovation Programme under Grant Agreement No 641185

In order to investigate the influence of this parameters in CO formation, two additional settings were tested during OF27 combustion: 20 and 40 Vol.% O_2. The measured CO profiles are presented in Figure 4-11. It is evident that CO formation is increased by reducing oxygen content in primary gas, indicating a strong activity of gasification reactions due to a high partial pressure of CO_2 in the center of the furnace. The reference red line appears considerably lower than the other two in the flame region. The differences become negligible toward the furnace outlet. From these observations it can be deduced that oxygen concentration in the primary gas can be used effectively to improve fuel ignition and CO formation in the near field area in order to obtain similar conditions as in air combustion.

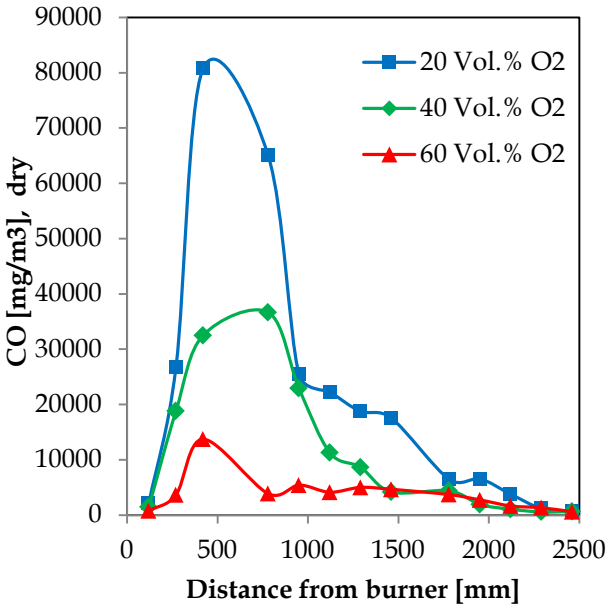

Figure 4-11: Measurements of CO (left) along the centerline of the furnace by variation of oxygen content in primary gas.

4.6 Effect of swirl angle

A usual parameter to adjust flame shape is the swirl angle. Primary gas was injected through an arrangement of 8 nozzles. A mechanism allows adjusting the angle of injection from 0° to 40°. By increasing the swirl angle a stronger mixing between fuel and oxidizer is fostered, which results in a shorter and more intense flame. This parameter has been useful to adjust flame formation when trying to obtain similar flame conditions as in air combustion.

As observed in Figure 4-12-left, when adjusting the swirl angle to 0° (straight flow), higher CO values are registered in a quite extended region. By increasing the swirl angle, the CO values reduce and temperature increases towards the burner (see Figure 4-12). Visually the flame became shorter and more stable.

This project has received funding from the European Union's Horizon2020 Research and Innovation Programme under Grant Agreement No 641185

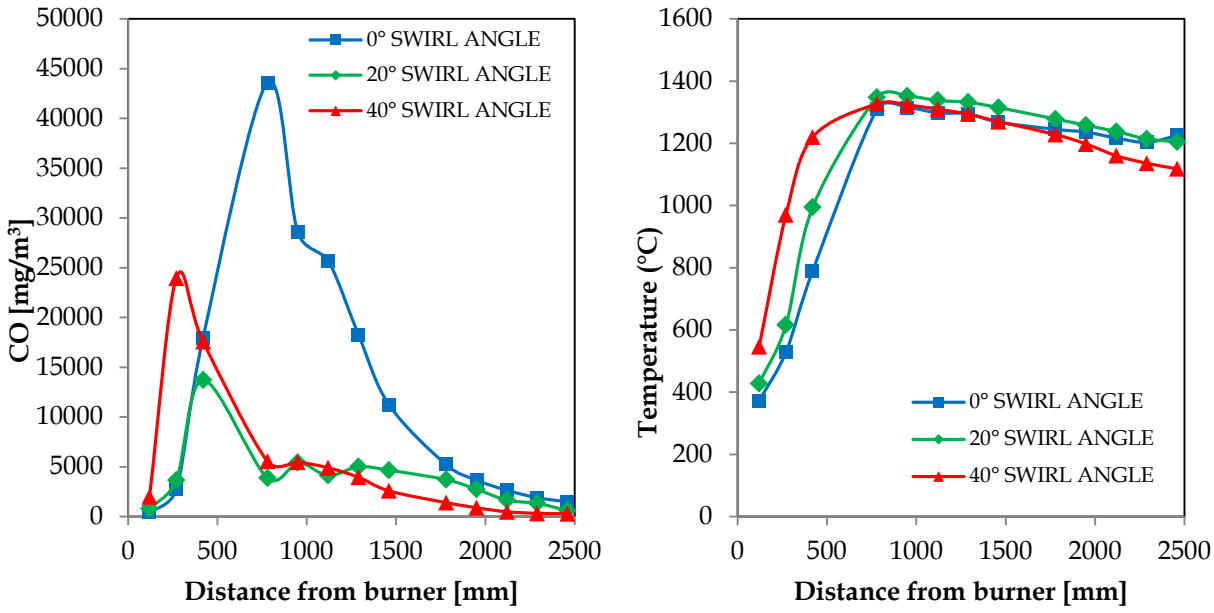

Figure 4-12: Effect of swirl angle adjustment in CO formation and temperature profile.

4.7 Air ingress effect

One of the main challenges of oxyfuel systems is the required tightness to avoid the entrance of undesired air to the process. The fan was operated under weak vacuum pressure to avoid the effect of drawing ambient air into the furnace through measurement ports and joints. However, air could be introduced to the system through an emergency air intake valve at the induced fan, which remained open in case of sudden CO_2 supply problems.

Figure 4-13 depicts the influence of an increase in oxygen concentration (due to air entrance) in CO_2 and NO emissions derived from gas concentration recordings during oxyfuel tests. When the oxygen concentration in flue gases increases in one percent due to air ingress, the CO_2 concentration drops 2-3%. As expected the NO concentration is increased when more air is allowed in.

This project has received funding from the European Union's Horizon2020 Research and Innovation Programme under Grant Agreement No 641185

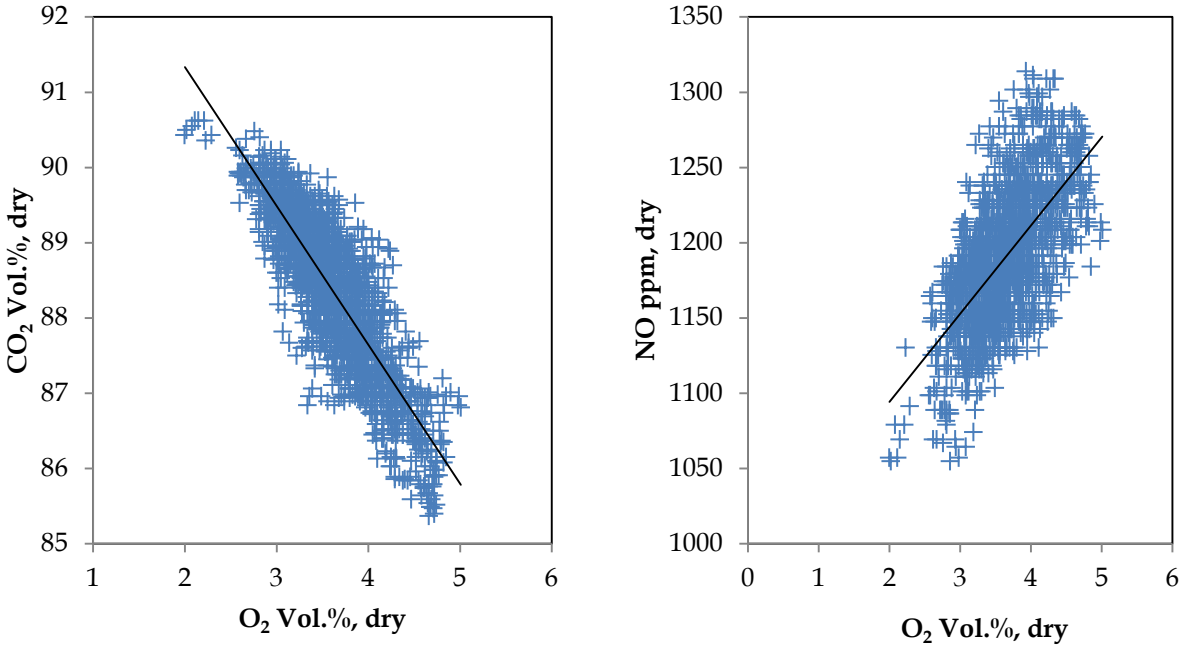

Figure 4-13: Effect of air entrance on CO_2 (left) and NO formation (right).

4.8 Fuel burnout

Fly ash from the electrostatic precipitator was sampled and analyzed to evaluate the efficiency of combustion. Fuel burnout was calculated using the following equation:

$$burnout = \frac{1 - \frac{\gamma_{ash,coal}}{\gamma_{ash,sample}}}{1 - \gamma_{ash,coal}}$$

Where $\gamma_{ash,coal}$ is the ash content of the dry fuel and $\gamma_{ash,sample}$is the ash content of the dry ash sample. As observed in Table 4-1 results from air and oxy-fuel combustion produced a good and comparable burnout percentage results.

Table 4-1 Calculated fuel burnout from fly ash.

	Air	**OF27**	**OF32**
Petcoke	98,2%	98,3%	97,4%
	Air	**OF29**	**OF32**
Pre-dried lignite	99,8%	99,8%	99,8%

By calculating the unburnt carbon it is also possible to assess the efficiency of combustion. The formula used to calculate this parameter is the following:

This project has received funding from the European Union's Horizon2020 Research and Innovation Programme under Grant Agreement No 641185

$$Unburnt\ carbon = \frac{y_{ash,coal}}{y_{ash,sample}} \cdot y_{c,sample}$$

Where $\gamma_{c,sample}$ represents the carbon content in the ash sample. The results are presented in Table 4-2, which shows that comparable values are obtained between air and oxyfuel cases. Higher unburnt carbon was found in combustion with petcoke, which values are considerably high compared to lignite values. The oxyfuel case OF32 produced higher unburnt carbon, which may appear confusing. However, the position of the burner and swirl were optimized for OF27 case, which possibly helped to increase combustion efficiency.

Table 4-2 Calculated unburnt carbon from fly ash.

	Air	**OF27**	**OF32**
Petcoke	1,72%	1,36%	2,29%
	Air	**OF29**	**OF32**
Pre-dried lignite	0,09%	0,11%	0,08%

4.9 Results with alternative fuels

Alternative fuels include a wide range of materials that may displace traditional fossil based fuels in cement kilns. Typically, they are differentiated by their origin in biomass derived fuels or mixed waste derived fuels. Solid Recover Fuel (SRF) is typically mixed waste derived fuel generated from municipal solid waste treatment plants. SRF is mainly composed of a mixture of non-recyclable paper, card, wood, textiles and plastic. Depending on the pretreatment system the size of SRF particles may vary in a range from 3 to 25 mm, several orders of magnitude larger than typical fossil fuel particles fired in cement kilns. Two samples of commercial SRF from different origin were analyzed at University of Stuttgart for fuel characterization purposes. As observed in Table 4-3, although different in origin, the analysis reveals a similar composition.

Table 4-3 Laboratory analysis of SRF sample (as received).

Fuel	**Moisture [wt. %]**	**Volatile Matter [wt. %]**	**Fixed Carbon [wt. %]**	**Ash [wt. %]**	**C [wt. %]**	**H [wt. %]**	**N [wt. %]**	**NCV J/g**
SRF-1	3,14	72,3	10,3	14,1	46,2	6,36	1,13	18955
SRF-2	4,91	70,5	8,94	15,6	45,1	6,68	1,07	17120

SRF-1: Provided by VDZ; SRF-2: Provided by REMONDIS GmbH Rheinland

The high volatile content is due to the proportion of plastics residues and foils in the mixture. This characteristic supports fast ignitions and self-sustaining combustion. The relative high net

This project has received funding from the European Union's Horizon2020 Research and Innovation Programme under Grant Agreement No 641185

calorific value (NCV) is close to typical NCV of lignite of about 22000 J/g. Currently many cement plants have substituted a large share of their fossil fuels for SRF even in the main burner due to the associated lower cost and carbon footprint reduction.

A particularity of SRF combustion lays in the aerodynamic behavior of the particles during entrained flow. Due to the non-sphericity of these particles modeling of such particle trajectories becomes a hard task. Furthermore, different to coal or petcoke, SRF particles undergo additional steps during early combustion stage, like shrinking. Under this premise, experiments are important to characterize the combustion behavior of such materials. Complementing the burner tests already done with conventional fuels (lignite and petcoke), additional tests with SRF in oxyfuel mode have been also performed. Due to downscaling constrains of burner and test facility, SRF particles were milled to a maximum of 1mm size in order to be burned properly. Even though the aerodynamic of the particles is most likely altered as well as the residence time in the furnace, useful information on flame characterization and gas emissions is valuable.

Burner demonstration tests using SRF

Co-firing tests of SRF with lignite were carried out in the 500kW$_{th}$ facility using the downscaled burner. The objective was to register differences in flame formation and emissions when modifying the combustion atmosphere (air vs. oxyfuel) and by increasing the oxygen content in primary gas. A summary of the test matrix is provided in Table 4-4.

Table 4-4 Burner tests summary of SRF co-firing with lignite

Test Case	Share of SRF [wt.%]	Oxygen share in primary gas [vol.%]
Air	20	21
OF30-a	20	50
OF30-b	20	20

In Figure 4-14 (left figure), the temperature profile over centerline is compared between two air test cases, one using 100 wt.% lignite from previous test campaign and a second partially substituting lignite with 20 wt% SRF (Air test case in Table 4-4). The composition of SRF used during these tests is presented in Table 4-3 as SRF-2. The co-firing tests with SRF presented a similar temperature profile over centerline as in air combustion but shifted towards the burner. This indication of sooner ignition is mainly attributed to a higher volatile content in total fuel mass. In real scale, however, ignition of larger particles could need longer distance.

When comparing the air test case (lignite + 20% SRF) against oxyfuel test cases (see Figure 4-14, right figure) very similar temperature profiles were observed despite differences in the oxidizing medium. Furthermore, among themselves both oxyfuel cases developed a similar profile over centerline with comparable peak temperatures. Apparently variations in oxygen proportion in primary gas have negligible influence on temperature profile over centerline for tested conditions. However, additional measurements over the furnace radius reveal some differences in flame formation. Figure 4-15 shows a temperature profile in a 2D plane obtained by interpolating 25 gas measurements distributed in the upper section of the combustion chamber up to a 2.4 m distance from burner outlet. A wider and longer flame is observed in the

This project has received funding from the European Union's Horizon2020 Research and Innovation Programme under Grant Agreement No 641185

oxyfuel test cases compared to the reference air case. These differences may be a result of differences in devolatilization and char burnout in oxyfuel systems.

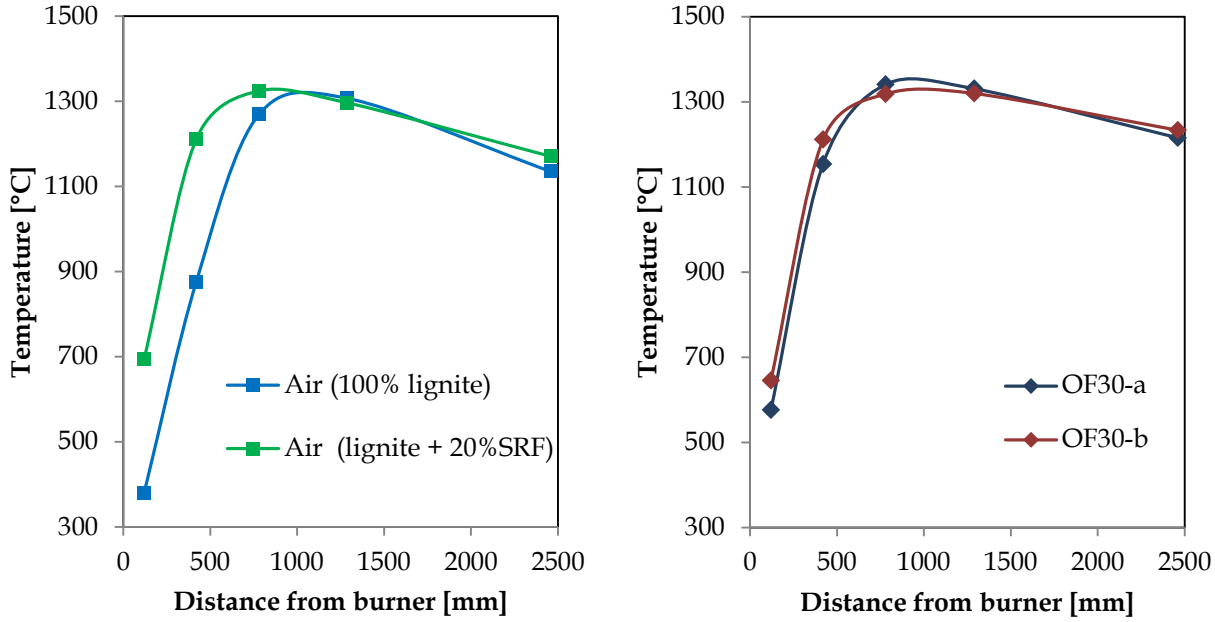

Figure 4-14: Temperature over centerline. Left: Influence of SRF addition under air firing. Right: Cofiring of Lignite and SRF in oxyfuel mode, variation of oxygen enrichment in primary gas.

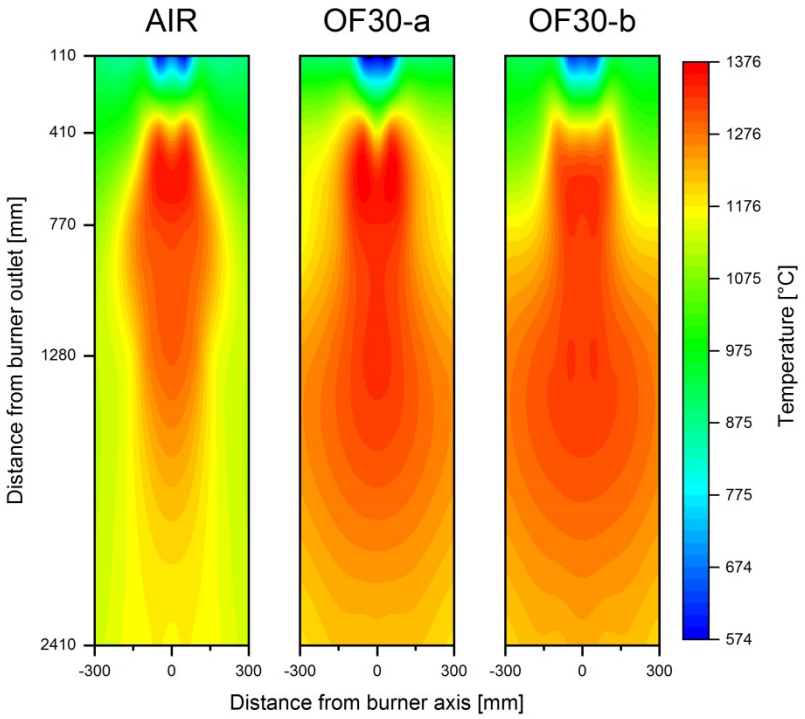

Figure 4-15: Temperature profile in a 2D plane by interpolation of 25 measurements.

The effect of oxygen enrichment in primary gas can be observed in Figure 4-16. Both the air case and the oxyfuel case with 50% vol.% of oxygen (OF32-a) present a similar CO distribution;

This project has received funding from the European Union's Horizon2020 Research and Innovation Programme under Grant Agreement No 641185

CO concentration increases with higher oxygen concentration (OF32-a) where fuel is ignited and is shortly after consumed. On the other hand, the oxyfuel case with only 20% oxygen in primary gas (OF32-b) presents significantly higher values of CO, which last longer to be consumed. This result is in line to the observed in Figure 4-11, an increase in oxygen enrichment in primary gas (oxygen share of 50% for OF32-a in Figure 4-16 and 60% in Figure 4-11) reduces the effects of CO production during oxyfuel combustion.

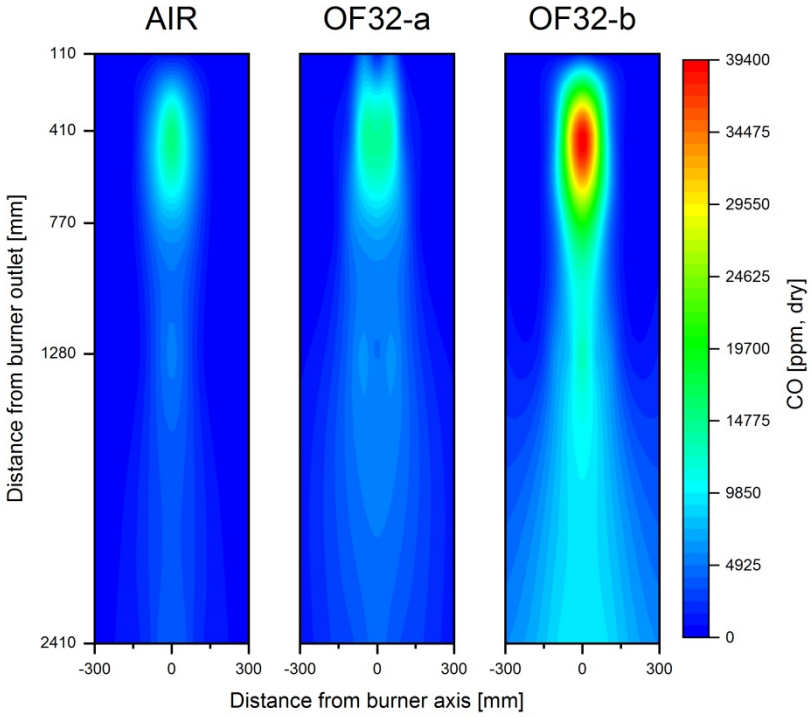

Figure 4-16: Carbon monoxide profile in a 2D plane by interpolation of 25 measurements.

Table 4-5 Flue gas composition and fuel burnout of SRF tests

	Unit	Air	OF32-a	OF32-b
O_2	vol.-%, dry	3,8	3,5	3,1
CO_2	vol.-%, dry	15,6	77,0	76,2
CO	ppm, dry	49	69	118
NO_x	ppm, dry	911	1713	1434
SO_2	ppm, dry	4	3	3
HCl	ppm, dry	28	62	49
Fuel burnout	%	98.8	99.1	98.8

Finally, flue gas composition at furnace outlet (see Table 4-5) shows that NO_x and HCl concentration increase during oxyfuel combustion. However, as shown previously in Figure 4-5, these values reduce significantly when expressed in mass over energy input. Ash samples near the furnace outlet were taken an analyzed to calculate fuel burnout. According to Table 4-5 no significant differences were found between the test cases.

This project has received funding from the European Union's Horizon2020 Research and Innovation Programme under Grant Agreement No 641185

5 INPUT DATA FOR WP6

One major objective of the burner technology work package is to provide input data to optimize the process modelling work of a full scale cement kiln retrofitted for oxyfuel. Information that could be exchanged include the following data:

- Flame length
- Flame shape
- Heat radiation to clinker bed
- Suggested primary/secondary volume flows and compositions

In order to find a way to transfer this information considering the constraints of extrapolating results from downscaled prototype investigations to full industrial scale, it was decided to implement a methodology for the transfer of results. Figure 5-1 indicates the pathway followed to transfer results from the demonstration tests with the burner prototype to the large scale process simulation in WP6:

Figure 5-1: Pathway to transfer results from prototype scale demonstration tests to WP6.

Results from the oxyfuel tests with the downscaled burner were used to obtain a set of experimental data that could be used in the following stage of the work package as validation data, i.e. simulation tools could be validated by comparing experimental data with calculated results from CFD simulations. Once CFD models were validated, a series of full scale kiln simulations were conducted to investigate an optimized oxyfuel case that would reproduce similar wall temperature and heat radiation to clinker bed profiles as in conventional combustion with air. The optimized oxyfuel case would then deliver the required input information to WP6.

For the purpose of generating validation data the following information from the 500kW tests has been shared with the simulation team:

- Experimental set up geometries. Furnace dimensions and detailed burner drawings were used for the creation of adequate simulation grids.
- Burner configuration (gas flows, temperatures, swirling). Different burner configurations were tested. Data regarding gas mass flows and temperatures, as well as swirl angle was shared.
- Fuel characterization. Fuel samples were analyzed in USTUTT laboratories to determine fuel composition and calorific value.
- Radial and axial profiles of gas temperature and concentration inside furnace. Numerous measurements were done at 15 different axial distances from furnace top. Moreover detailed radial measurements every 5 cm complemented the information to create detailed profiles.
- Wall radiation and heat flux measurements

Besides the generation of validation data sets, demonstration tests provided additional insights regarding the differences between combustion in CO_2/O_2 and conventional air combustion in

This project has received funding from the European Union's Horizon2020 Research and Innovation Programme under Grant Agreement No 641185

conditions similar to clinker production. This information is valuable and could be qualitatively considered during up-scaling of oxyfuel burners. Some of this information includes:

- **Differences in gas temperature**. As highlighted in Section 4.3, an oxyfuel case with oxygen concentration higher than 27 vol.% produces a higher temperature profile than air combustion. The peak temperature is shifted towards the burner, while further downstream the differences are reduced significantly.
- **Differences in heat transfer**. Radiative heat transfer to furnace wall is observed to be significantly influence by flame temperature. Oxyfuel cases with higher flame temperature than air firing produce higher radiative heat flux (see Section 4.4). Similar radiation profile as in air combustion could be replicated with an oxyfuel case with oxygen enrichment slightly lower than 25 vol.%.
- **Influence of oxygen enrichment in primary gas**. By increasing oxygen volume proportion in primary gas the formation of CO in the near burner area is reduced (see Figure 4-11), replicating a similar behavior as in air combustion.

This project has received funding from the European Union's Horizon2020 Research and Innovation Programme under Grant Agreement No 641185

6 CONCLUSION

In this work the downscaling of a modern high momentum jet burner for testing under oxyfuel conditions has been presented. The performance of the downscaled burner was evaluated with petcoke, lignite and in co-combustion with up to 20 wt-% SRF in a combustion rig adapted for oxyfuel combustion with secondary gas preheating. Fuel has been burned under air and oxyfuel conditions in order to assess the differences in combustion behavior, emissions and fuel burnout in rich CO_2 atmosphere. After assessment of in-flame measurements it has been established that the prototype burner is suitable for oxyfuel operation considering that similar temperature and heat flux profiles can be replicated as in air operation. This means that the modern high momentum burners with single jets could be employed for oxyfuel operation without extensive modifications. It has been observed that flue gas recycle ratio i.e. oxygen concentration in input gases is the main parameter to influence temperature and radiation profile. By adjusting the overall oxygen content near 27 vol.% in oxyfuel mode similar temperature and heat flux results were obtained in CO_2/O_2 and air firing conditions. Important is to note that by increasing the oxygen content to this extend the volume of combustion gases is reduced and the possibility to operate the preheater cyclones must be carefully examined.

Oxygen distribution in burner outlets was also found to be a key parameter to improve ignition behavior and CO formation in the near burner region. The tests indicated that by increasing oxygen content up to 60%, CO production remains in similar levels as in air combustion. Finally, swirling flows continue to be a recommended tool to shape flame formation and adjust flame length when changing combustion conditions.

The results have been used for validation purposes of CFD combustion models with the goal to simulate an oxyfuel burner in a large scale rotary kiln. The results of those simulations are presented in Deliverable 7.3. Likewise required information has been exchanged with work package 6 in order to improve the quality of input parameters fed to process modeling.

This project has received funding from the European Union's Horizon2020 Research and Innovation Programme under Grant Agreement No 641185

A LITERATURE

[1] ECRA, ‘Report on Phase III. ECRA CCS Project’, European Cement Research Academy, Düsseldorf, Germany, Technical Report TR-119/2012, 2012.
[2] L. D. Smoot, S. C. Hill, and H. Xu, ‘NOx control through reburning’, *Progress in Energy and Combustion Science*, vol. 24, no. 5, pp. 385–408, Oct. 1998.
[3] C. Ndibe, R. Spörl, J. Maier, and G. Scheffknecht, ‘Experimental study of NO and NO2 formation in a PF oxy-fuel firing system’, *Fuel*, vol. 107, pp. 749–756, May 2013.
[4] B. Dhungel, ‘Experimental Investigations on Combustion and Emission Behaviour during Oxy-Coal Combustion’, IFK, University of Stuttgart, Stuttgart, 2009.

This project has received funding from the European Union's Horizon2020 Research and Innovation Programme under Grant Agreement No 641185